Development and characterisation of reparable, film-interleaved, pseudo-ductile hybrid composites

Marino S. G., Czél G.

Composites: Part A 169 (2023) 107496

Contents lists available at ScienceDirect

Composites Part A

journal homepage: www.elsevier.com/locate/compositesa

Development and characterisation of reparable, film-interleaved, pseudo-ductile hybrid composites

Salvatore Giacomo Marino, Gergely Czél *

Department of Polymer Engineering, Faculty of Mechanical Engineering, Budapest University of Technology and Economics, Műegyetem rkp. 3, H-1111 Budapest, Hungary

ARTICLE INFO

Keywords:
A. Hybrid
B. Fracture toughness
Reparability
Pseudo-ductility

ABSTRACT

The recent developments in pseudo-ductility demonstrated the possibility of making composites safe and suitable for high-performance applications. Repairing damage in composites is an attractive challenge for the industry, as it may increase the reliability of composites and reduce the waste generated by components damaged locally. In this paper, we interleaved polyamide 12 (PA12) films in discontinuous carbon/epoxy – continuous glass/epoxy hybrid composites to i) increase their interlaminar toughness and make them more damage tolerant, and ii) repair delamination damage by heating the samples and exploit the re-bonding feature of the thermoplastic interleaves. The developed repairing method successfully restored the original pseudo-ductile behaviour in the tested hybrid laminates. We studied the parameters affecting the repairing process to maximise the repairing efficiency. We present the design process in detail to ease the introduction of reparable pseudo-ductile composites in the industry.

1. Introduction

Fibre-reinforced polymer composites (FRPC) are lightweight and high-strength materials suitable for high-performance structural applications. However, composites' potential is not fully exploited because of their brittleness and low damage tolerance against delamination, issues that limit their safety in practical applications. Hybridisation has been demonstrated to i) provide composites with a safety margin before the final failure and ii) enable pseudo-ductility, which makes composites able to mimic the nonlinear stress–strain response of metals. The technical literature offers a number of design solutions to achieve pseudo-ductility in carbon/glass–epoxy composites [1–7]. Pseudo-ductile composites made with a discontinuous carbon/epoxy layer (i.e. low-strain material – LSM) between continuous glass/epoxy layers (high-strain material – HSM), were studied in [3]. The discontinuous/continuous architecture is suitable for enabling pseudo-ductility based on the stable delamination between the discontinuous carbon fibre/epoxy (CF/EP) platelets and the continuous glass fibre/epoxy (GF/EP) layers.

Delamination seriously compromises the material's ability to withstand loads, but recent studies on self-healing materials showed that composites can recover from delamination and restore degraded mechanical properties by exploiting the effect of a healing agent [8–10]. Thermoplastic polymers (TPP) are excellent candidates for repairing delamination and making the repair process repeatable [11,12]. Furthermore, TPP particles, fibres or films can introduce beneficial toughening effects and make composites more damage tolerant [13,14,23,24,15–22]. The combination of high temperature and pressure allows TPPs to spread and penetrate cracks in the matrix and delaminated zones in damaged composite material and eventually re-bond the separated surfaces. It is common in the literature to refer to reparable composites using the keyword "self-healing" [25], although it would imply the materials' ability to recover autonomously from damage [26]. In practice, especially when TPPs are employed as a reparable component (sometimes called "healing or repair agent"), materials require an external stimulus [25], e.g. heat, to trigger and maintain the repairing process. For this reason, we find the term "reparability" more appropriate for referring to composites that require external intervention for initiating and completing a repairing process based on phase transitions of TPP components.

Wang et al. [15] repaired carbon/epoxy composites containing patches of thermoplastic copolymers. Furthermore, the presence of the patches promoted toughening effects that resulted in a higher mode I interlaminar fracture toughness (G_{IC}) for the interleaved material compared to the control configuration (i.e. without patches). The

* Corresponding author.
E-mail addresses: marinos@pt.bme.hu (S.G. Marino), czel@pt.bme.hu (G. Czél).

https://doi.org/10.1016/j.compositesa.2023.107496
Received 28 November 2022; Received in revised form 31 January 2023; Accepted 18 February 2023
Available online 23 February 2023

repairing efficiency for G_{IC} was up to 88% in the composites containing the copolymer poly(ethylene-co-methacrylic acid) (EMAA). Pingkarawat et al. [11] mixed 15% ground particles of EMAA within the matrix of carbon fibre reinforced composite, which formed a phase-separated blend with uniform EMAA particle distribution. Besides the higher G_{IC} in the configuration containing EMAA particles, the repairing efficiency for G_{IC} was up to 210% after the first repairing cycle, and it remained above 200% in the successive five repairing cycles compared to the pristine baseline. The repairing mechanisms promoted by TPPs vary in function of the interaction between the components. The EMAA/epoxy system can produce volatilities that generated bubbles in the TPP phase [27,28]. At high temperatures, bubbles expanded and pushed the melted EMAA into the damaged regions and effectively re-bonded the damaged zones [11,15,21,27,29]. The dominant adhesion mechanism between epoxy and EMAA was based on hydrogen bonding [27]. The microscope analysis in [29] revealed that the high repairing efficiency was related to the diffused bridging ligaments created by the TPP component in the damaged zones. The bridging effect is also typical for ethylene–vinyl acetate (EVA), as confirmed by several studies [11,17–21]. Varley et al. [29] also identified EVA as an effective agent for repairing epoxy matrices, as the low viscosity at the typical repair temperatures around 150 °C allowed for a good distribution of the agent, even in small cracks.

The reparability concept has been implemented in open-hole notched composites by using thermoplastic polyurethane (TPU) films in CF/EP laminates locally around the holes [30]. The TPU films repaired delamination in the samples after tensile tests. Also, it was shown that the approach was effective for repairing matrix cracks and local delamination due to drilling operations for making holes in the composite.

Still, there are limited examples of direct application of reparable composites in industry, mainly due to the complexity of the design and manufacturing [31,32]. Therefore, there is space for new, simpler concepts of reparable composites which can be easily integrated into existing manufacturing processes. Furthermore, adding reparability to pseudo-ductile composites as an additional function may increase their attractiveness for demanding applications.

2. Concept and design

Unidirectional (UD) pseudo-ductile hybrid composites can be made by sandwiching discontinuous CF/EP plies between two GF/EP layers. Under tensile loads, they can generate pseudo-ductility through the stable delamination of the CF/EP platelets from the GF/EP layers [3]. The reparability concept reported in this paper is schematically shown in Fig. 1, and it concerns the possibility of recovering composites from delamination and restoring their original pseudo-ductile behaviour. Delamination is repaired by softening/melting polyamide 12 (PA12) TPP films inserted between the CF/EP and GF/EP layers, where delamination takes place. The layer thicknesses, the discontinuity pattern and the position of the interleaves was determined through careful material architecture design. This way, the TPP films can restore the bonding between the fibre-reinforced layers after severe delamination damage accumulation.

Some of the design aspects and the mechanisms enabling pseudo-ductility in the discontinuous/continuous layer hybrid composites were discussed by Czél et al. in [3]. The key design parameters controlling the material's performance are i) the platelet length (L_p), that has to be higher than the critical (or ineffective) length (L_{pc}, see inequality (2.1)) to enable effective stress transfer to the high modulus LSM platelets and useful contribution to the hybrid laminate stiffness, ii) the thickness of the GF/EP (t_g) and CF/EP (t_c) layers controlling the mode II strain energy release rate (G_{II}) and iii) the mode II interlaminar fracture toughness (G_{IIC}), as showed in equation (2.2) [3]. The thicknesses t_c and t_g and the G_{IIC} are used to predict the knee-point (kp) stress σ_{kp} (graphically defined in Fig. 3), i.e. where stable delamination between the CF/EP platelets and the GF/EP layers initiate.

$$L_p > L_{pc} = \frac{E_c t_c \varepsilon_c^f}{\tau_s} \tag{2.1}$$

$$\sigma_{kp} = \sqrt{\frac{8E_g t_g \left(2E_g t_g + E_c t_c\right) G_{IIC}}{h^2 E_c t_c}} \tag{2.2}$$

E_g and E_c are the elastic moduli of the CF/EP and GF/EP layers, respectively; ε_c^f is the failure strain of the CF/EP; τ_s is the interfacial shear strength of the PA12 film modified CF/EP and GF/EP layer interfaces; h is the total thickness of the laminate.

In general, the material needs to meet the following criteria:

1. Avoid premature failure of the GF/EP layers and guarantee the complete delamination of the CF/EP platelets in the hybrid composites. Formula (2.3) can be used for a conservative estimation of the minimum thickness of the GF/EP layer in function of the strain to failure of the CF/EP (ε_c^f) and GF/EP (ε_g^f) layers [1,3]. The condition for the formula assumes no delamination and that the full load at carbon layer failure stain has to be taken by the glass layers only. This is clearly conservative as the material architecture is designed for delamination initiation well before CF/EP failure strain, therefore the stress in the glass layer will remain below the design limit until high strains.

$$t_g > \frac{\varepsilon_c^f E_c t_c}{2E_g\left(\varepsilon_g^f - \varepsilon_c^f\right)} \tag{2.3}$$

2. Avoid fracture or fragmentation of the CF/EP layer; only delamination should take place in the specimens before final failure. This requires a configuration where the mode II strain energy release rate (G_{II}) at CF/EP layer failure strain is higher than the interlaminar fracture toughness (G_{IIC}) of the interface between the CF/EP and GF/EP layers [3]. This criterion is expressed by inequality (2.4).

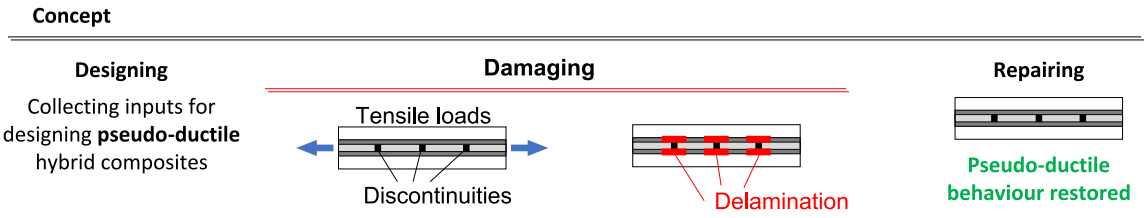

- Hybrid composites interleaved with thermoplastic films.
- Enabling reparability through heat and pressure.
- Re-bonding delaminated interfaces to restore the original pseudo-ductility.

Fig. 1. Concept implemented in this study for repairing delamination.

$$G_{II@CF/EPfracture} = \frac{\varepsilon_c^f E_c t_c (2E_g t_g + E_c t_c)}{8E_g t_g} > G_{IIC} \quad (2.4)$$

The hybrid composites used in this paper were interleaved with PA12 films with the scope of i) increasing the material's mode II fracture toughness and ii) repairing delamination. To design a suitable material architecture (i.e. predict delamination stress, determine the suitable length of the CF/EP platelets, and select the thicknesses of the fibre reinforced layers), we needed the G_{IIC} and τ_s of the interleaved composites. Since these parameters are not available in the literature or in manufacturer's datasheets, we estimated them through simple tensile tests on special specimen configurations designed to produce the desired loading and failure modes. A schematic overview of all hybrid composite configurations used in this study is reported in Fig. 2. The specimen architecture used to estimate the G_{IIC} and the τ_s is shown in Fig. 2 (a) and (b), i.e. central-cut carbon/epoxy and double-lap shear configurations, respectively. The central-cut architecture used for estimating the G_{IIC} was presented in [33] for GF/EP and it was adapted here to hybrid composites. The results of the G_{IIC} and the τ_s estimation tests are presented in section 4.1, where the discontinuous, interleaved hybrid laminate configuration designed for the reparability study is introduced as well.

The experiments for studying reparability in pseudo-ductile composites were executed on specimens whose architecture is shown in Fig. 2 (c), i.e. with discontinuous carbon/epoxy platelets. An analysis of the key repairing process parameters, i.e. pressure and temperature, has been carried out to find the optimal conditions for repairing delamination (see sections 4.3 and 4.4).

3. Materials and methods

3.1. Materials

The UD prepregs of IM7 carbon/913 epoxy and S-glass/913 epoxy

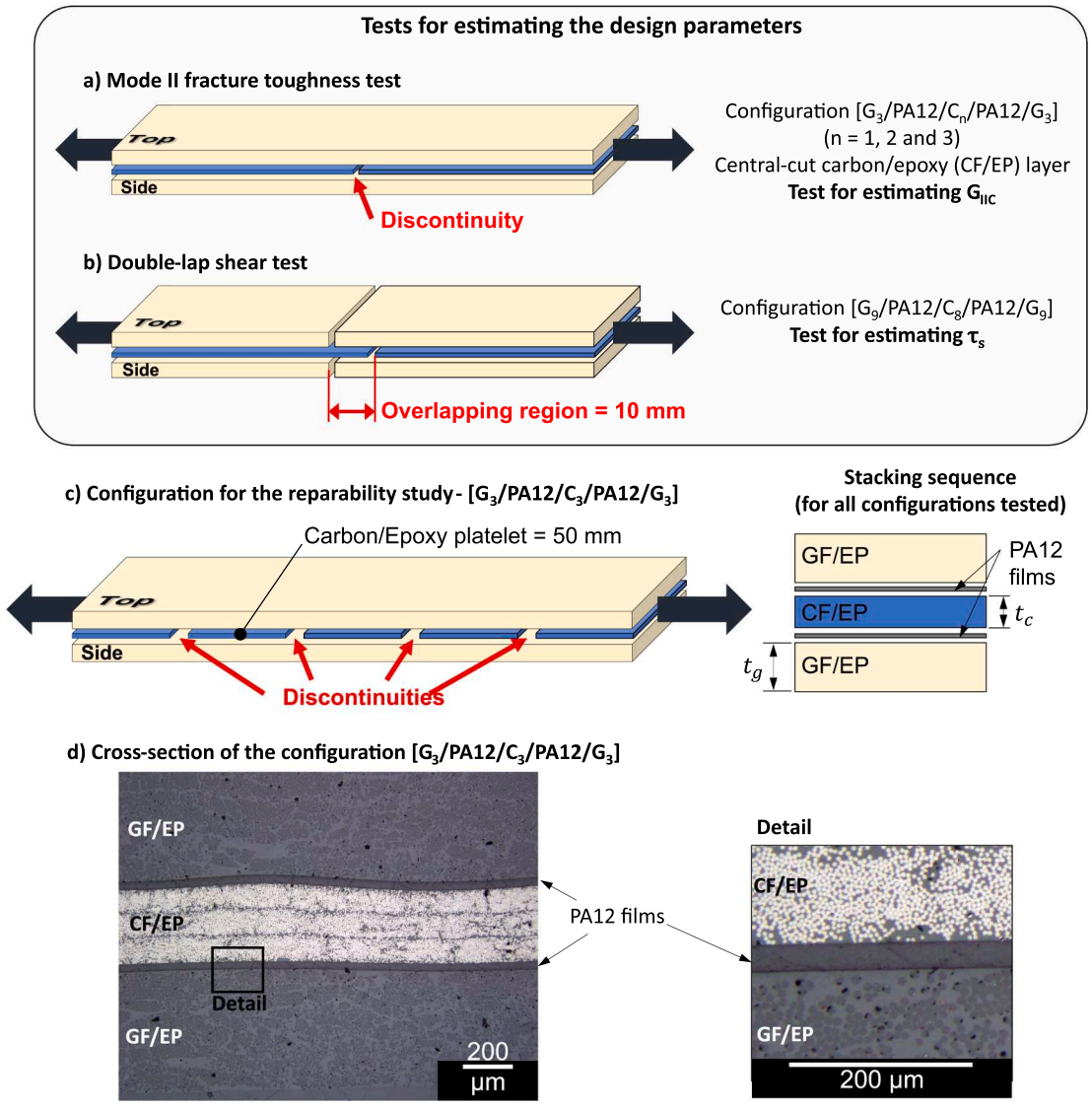

Fig. 2. Unidirectional (UD) material configurations and layup architectures of the hybrid composites used in the experiments: a) central-cut hybrid laminate, b) double-lap shear specimen, c) discontinuous carbon/epoxy and continuous glass/epoxy hybrid laminate d) shows the cross-sectional optical microscope view of the configuration used for the reparability study.

Table 1
Basic properties of the applied UD composite prepregs based on manufacturer's data.

Prepregs	Nominal fibre areal density [g/m^2]	Fibre volume fraction [–]	Cured ply thickness [μm]	Tensile elastic modulus [GPa]	Tensile strain to failure [%]
AGY Y-110 S-2 Glass/913 epoxy	190	0.49	153.8	45.6	3.7[(a)]
Hexcel IM7 Carbon/913 epoxy	100	0.58	95.8	163.2	1.6

[(a)] Conservative strain limit based on our tests on pure S-glass/epoxy and hybrid specimens.

Table 2
Mechanical and thermal properties of the polyamide 12 (PA12) used to make thin films.

	Density [g/cm^3]	Nominal film thickness [μm]	Elastic modulus [GPa]	Tensile strength [MPa]	Elongation at break [%]	Melting temperature [°C]
Grilamid L25 PA 12	1.01	20	1.1	50	> 50	178

were both supplied in 300 mm wide rolls by Hexcel. The key properties of the materials are reported in Table 1.

We produced the polyamide 12 (PA12) film by film blowing Grilamid L25 (EMS-Grivory) PA12 pellets with a Labtech LF-400 type extruder. The temperature of the extruder zones was in the range of 210–230 °C. The nominal thickness of the resulting PA12 films was set to 20 μm. The basic properties of PA12 are reported in Table 2.

3.2. Hybrid composite laminate manufacturing

The hybrid composite laminates were manufactured by sandwiching UD prepreg sheets of IM7 carbon fibre/913 epoxy between PA12 films and UD S-glass fibre/913 epoxy prepregs (see Fig. 2 (c)). All UD prepreg plies were stacked together with the same fibre orientation aligned to the tensile loading direction. The stacking sequence is shown in Fig. 2 (c). The structure of the hybrid laminates was similar for all three material architectures reported in Fig. 2, the main difference was in the number of CF/EP and GF/EP plies and the continuity of the CF/EP layer. The hybrid laminates were cured in an Olmar ATC 1100/2000 type autoclave at 125 °C and 0.7 MPa for 60 min, according to the prepreg manufacturer's recommendation. A 0.095 MPa vacuum was applied after sealing the vacuum bag and during the initial pressurisation phase in the autoclave. However, the vacuum was switched off after the pressure in the autoclave exceeded 0.12 MPa. The test specimens were fabricated by cutting the composite plates with a diamond cutting wheel. The nominal dimensions of the samples were 260x20 mm (nominal full length/width, respectively). 50 mm sections were gripped, so the resulting nominal free length of the samples was 160 mm. The manufacturing quality of the samples was assessed through microscope analysis (see Fig. 2 (d)). The PA12 films maintained a uniform thickness along the cross-section of the samples. We did not notice the presence of air bubbles entrapped between the fibre reinforced layers and the thermoplastic films.

3.3. Microscope analysis

The material's cross-section was analysed with an Olympus BX51M type optical microscope (Olympus, Germany). For this purpose, representative parts of the pristine laminates were cut with a diamond wheel and then embedded in epoxy that was crosslinked for 24 h at ambient temperature. The resin blocks were polished with a Buehler Beta type machine with sandpapers (grit size P350 and P1000) and liquid suspensions of 9, 3 and 0.05 μm abrasive particles.

3.4. Mode II fracture toughness estimation test

The mode II interlaminar fracture toughness (G_{IIC}) of the film modified CF/EP-GF/EP interfaces was estimated through a tensile test on UD hybrid laminates made with a central-cut CF/EP layer (see configuration in Fig. 2 (a)). The cut in the CF/EP layer promoted mode II deformations (i.e. shearing) and initiated delamination between the CF/EP and GF/EP layers, where the PA12 films were placed. The layup stacking sequence of the UD hybrid material for the G_{IIC} estimation test was [G_3/PA12/C_n/PA12/G_3], where G indicates the GF/EP plies and C the CF/EP plies. The subscripts indicate the number of plies used in the layer (e.g. G_3 has three plies of GF/EP in one block). The specimens for estimating the G_{IIC} were designed to avoid fragmentation of the CF/EP layer (i.e. G_{II} at CF/EP layer failure strain was set to be higher than G_{IIC}) as the scope of the test is to promote delamination between the CF/EP and the GF/EP layers and estimate the energy required for its initiation and propagation. Since we presented the estimated G_{IIC} = 2 kJ/m^2 of the non-interleaved configuration [G_3/C/G_3] previously in [14] determined with the same test method, this was considered as a baseline. Therefore, we tested its interleaved version first for a direct indication of the toughening effect of the TPP interleaves. However, we needed to increase the number of CF/EP pies to two and finally to three, while keeping the number of GF/EP plies the

Table 3
Configurations and dimensions of the hybrid samples used for the fracture toughness estimation test. Coefficient of variation (CoV) in % expressed in brackets below the mean values.

Central-cut CF/EP layer configurations for G_{IIC} estimation tests	Lay-up sequences	Nominal thickness of the CF/EP layer $t_{CF/EP}$ [mm]	Nominal thickness of the GF/EP layer $t_{GF/EP}$ [mm]	Measured thickness h [mm]
Hybrid layup - without film interleaves (Baseline configurations) [14]	[G_3/C/G_3]	0.10	0.47	1.09 (2.00)
Hybrid layups - containing PA12 film interleaves (Interleaved configurations)	[G_3/PA12/C/PA12/G_3]	0.10	0.47	1.01 (1.17)
	[G_3/PA12/C_2/PA12/G_3]	0.19	0.47	1.21 (1.69)
	[G_3/PA12/C_3/PA12/G_3]	0.29	0.47	1.29 (1.46)

same, to get pure delamination between the layers due to the superior fracture toughness of the PA12 interleaved interfaces. The list of all tested configurations is reported in Table 3.

The G_{IIC} from the test results of central-cut CF/EP layer hybrid specimens was estimated using formula (3.1) [13]. The delamination onset stress (i.e. σ_{del}) was determined at the intersection of the experimental curves and lines having 1% reduced slope compared to the lines fitted to the initial linear elastic regime of the stress–strain curves.

$$G_{IIC} = \frac{\sigma_{del}^2 h^2 E_c t_c}{8E_g t_g \left(2E_g t_g + E_c t_c\right)} \tag{3.1}$$

3.5. Interfacial shear strength estimation tests

The interfacial shear strength of the CF/EP – GF/EP layer interfaces was estimated through a double-lap shear test. The architecture of the specimens used for this test is shown in Fig. 2 (b). The layup sequence for the double-lap shear test was [G_9/PA12/C_8/PA12/G_9]. The thicknesses of the CF/EP and GF/EP layers were chosen to have the same stiffness in both layers (the two GF/EP layers designed to have similar stiffness as that of the CF/EP layer). The layer thicknesses are also made sufficient to avoid premature fracture of the layers at the discontinuities during the tensile test. The length of the overlapping region (see Fig. 2 (b)) was set to 10 mm according to equation (2.1), to be lower than the ineffective length of the 8 plies thick CF/EP layer calculated using a conservative value of interfacial shear strength of 100 MPa, reported for glass fibre/

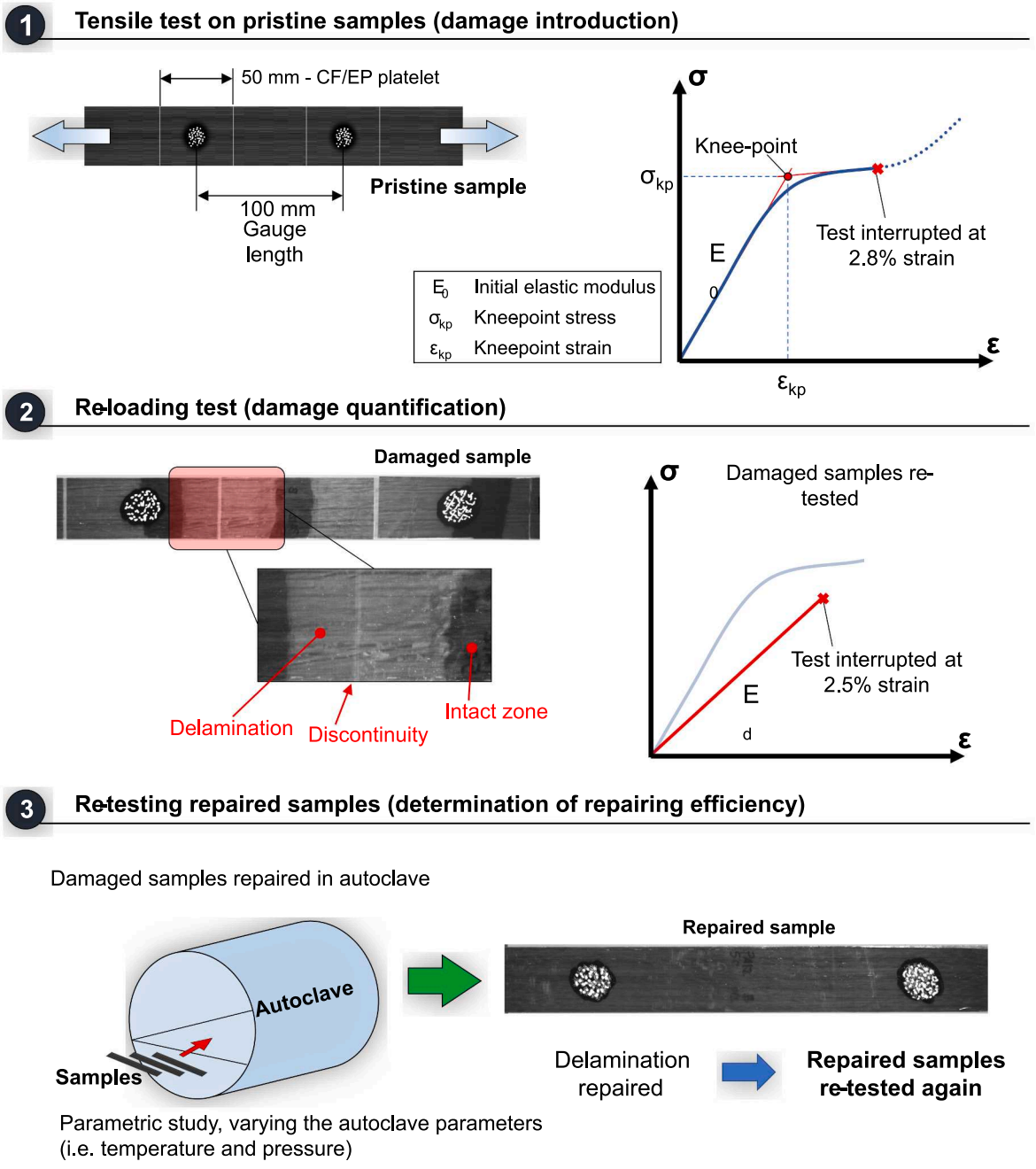

Fig. 3. Test steps performed in the experimental campaign for studying the reparability of hybrid samples.

913 epoxy [34]. This way, we eliminated the risk of fracture of the fibres during the test. The value of the ineffective length related to 8 plies thick CF/EP layer was 23.8 mm. The gauge length used to measure strain in the samples was 120 mm.

3.6. Specimens and tensile test procedure for the reparability study

The uniaxial, quasi-static tensile tests on all type hybrid composite laminates (including the special specimens for G_{IIC} and the τ_s estimation) were conducted on a computer-controlled Zwick Z250 universal electro-mechanic test machine, fitted with a regularly calibrated 250 kN load cell and 100 kN rated Instron 2716–003 type manual wedge action grips with similar parameters. The crosshead displacement speed was set to 5 mm/min. The high strain S-glass/epoxy layers on the outside of the hybrid laminates allowed to test the specimens without using end-tabs, as demonstrated in [35]. However, the two ends of the specimens were covered with 50 mm long P80 grit size sandpaper pieces with the rough side turned to the specimen surface to prevent damage from the sharp nails of the grip faces while maintaining sufficient friction to avoid slippage. The strain was measured with a Mercury RT type optical extensometer system equipped with a 5 MPixel Mercury Monet camera (Sobriety, Czech Republic). The gauge length of the specimens (i.e. the distance between the markers tracked by the extensometer) was set to 100 mm (see Fig. 3) to the centre of two CF/EP platelets.

The experimental procedure for studying the reparability of the hybrid laminates involved three tensile tests on each specimen to measure the mechanical properties i) before and ii) after damage introduction (i.e. delamination), and iii) after the repairing cycle. The hybrid specimens for the reparability study had a discontinuous CF/EP layer, i.e. CF/EP platelets, as shown in Fig. 2 (c). The length of the CF/EP platelets (L_p) was selected following the guidelines reported in [3], setting L_p two times higher than the ineffective length of the CF/EP layer, calculated as per equation (2.1). Before proceeding with the tests on the samples dedicated to the reparability study, we tested six discontinuous hybrid samples until final failure to compare the measured mechanical properties of the material with the predicted values.

The tensile test sequence of the reparability study was the following:

- ***First loading test (step 1)***: The first tensile test on the specimens had the aim to i) measure the mechanical properties of the pristine specimens and ii) introduce damage (i.e. delamination) to the specimens. The test was interrupted at 2.8% of strain to avoid the failure of the glass fibres. The elastic modulus (E_0) and the knee-point strain (ε_{kp}) and stress (σ_{kp}) were evaluated based on this first test (see Fig. 3, part 1).
- ***Re-loading test (step 2)***: After the *first loading test*, the damaged specimens were re-tested to measure the reduced stiffness of the damaged material. It is worthwhile to note that the elastic modulus after damage introduction E_d is not a material property as it depends on the extent of the introduced damage i.e. on how extensively the delamination spread in the previous step (basically at what strain the *first loading test* was stopped at). E_d is determined to quantify the damage (i.e. stiffness loss) in the samples. This test was interrupted at 2.5% strain to prevent the samples from further delamination propagation (see Fig. 3, part 2).
- ***Test on repaired samples (step 3)***: The repaired samples were tested the same way as during the *first loading test*. The resulting elastic modulus, knee-point strain and knee-point stress were compared to those of the pristine specimens (i.e. evaluated after the *first loading test*). The repairing efficiency (η) is calculated as the ratio of the repaired ($P_{repaired}$) and pristine ($P_{pristine}$) mechanical parameters of the material (see equation (3.2)). Part 3 of Fig. 3 summarises this test.

$$\eta = \frac{P_{repaired}}{P_{pristine}} \tag{3.2}$$

Table 4
Parameters used for the repairing cycles.

Series designation	**Temperature** [°C]	**Pressure** [MPa]	**Time at max. temp.** [min]
T165	165	0.7	13
T175	175	0.7	16
T185	185	0.7	14
P4	185	0.4	15
P6	185	0.6	14
P8	185	0.8	15

The knee-point is considered as an indication of delamination initiation, and it is used here to assess the ability of the PA12 films to re-bond the delaminated surfaces through the repairing cycles. The scheme reported in Fig. 3 (see diagram in part 1) graphically defines the parameters used for characterising the mechanical performance of the specimens and for calculating the repairing efficiency.

3.7. Repairing cycles

The delaminated samples were repaired in the autoclave (Fig. 3 – part 3). We studied the effect of different autoclave parameters (i.e. temperature and pressure) on the repairing efficiency. Table 4 lists the six repairing conditions applied to six series of samples. Four samples per series have been repaired and tested. The series are named according to the parameter varied in the repairing cycles, e.g. T165, T175 and T185 for the cycles where the temperature was 165 °C, 175 °C and 185 °C, respectively; similarly for pressure.

4. Results

4.1. Estimation of the key design parameters

The G_{IIC} estimation tests were performed on the central-cut hybrid layups containing PA12 films (see Fig. 2 (a)). The configurations [G_3/PA12/C/PA12/G_3] and [G_3/PA12/C_2/PA12/G_3] exhibited fragmentation of the CF/EP layer, as shown in Fig. 4 (a.1) and (a.2). Therefore, these two configurations were not suitable for estimating the G_{IIC} of the GF/EP and CF/EP layer interfaces. The presence of fragmentation meant that the thickness of the CF/EP layer was not high enough to satisfy inequality 2.4, i.e. to initiate delamination before CF/EP layer fracture. This means that the presence of the PA12 films made the hybrid laminates significantly tougher than the non-interleaved hybrid configuration [G_3/C/G_3], which exhibited delamination and had a G_{IIC} of 2.0 kJ/m^2 (see Fig. 4 (a.4)). The experimental results of the tests on the layup [G_3/PA12/C_3/PA12/G_3] are reported in Fig. 4 (b). This configuration exhibited delamination only (see Fig. 4 (a.3)) and the test was suitable for evaluating the G_{IIC} of the interleaved hybrid material. The G_{IIC} is compared to the one estimated for the baseline configuration without film interleaves. Since the baseline and the interleaved hybrid laminates were made of the same materials (both fibres and matrix), but with slightly different layup sequence (thicker CF/EP was needed to make the interleaved specimens work) their results are still considered comparable and suitable to assess the effect of the PA12 films on the mode II fracture toughness of the laminates.

The σ_{del} obtained from the tests on the PA12 interleaved configurations was 883 MPa and the G_{IIC}, calculated through equation (3.1), was 4.0 kJ/m^2. The results show that G_{IIC} increased from the reference value of 2.0 kJ/m^2 (obtained from the baseline configuration) to 4.0 kJ/m^2 for the hybrid composites containing PA12 films. This is a notable, more than two-fold increase which is considered beneficial on its own to promote the pseudo-ductility of hybrid composites.

The interfacial shear strength (τ_s) between the GF/EP and the CF/EP layers (i.e. where the PA12 films were inserted) was estimated through double-lap shear tests. The test results are reported in Fig. 4 (c). The two halves of the samples separated at around 36 MPa stress, exhibiting a

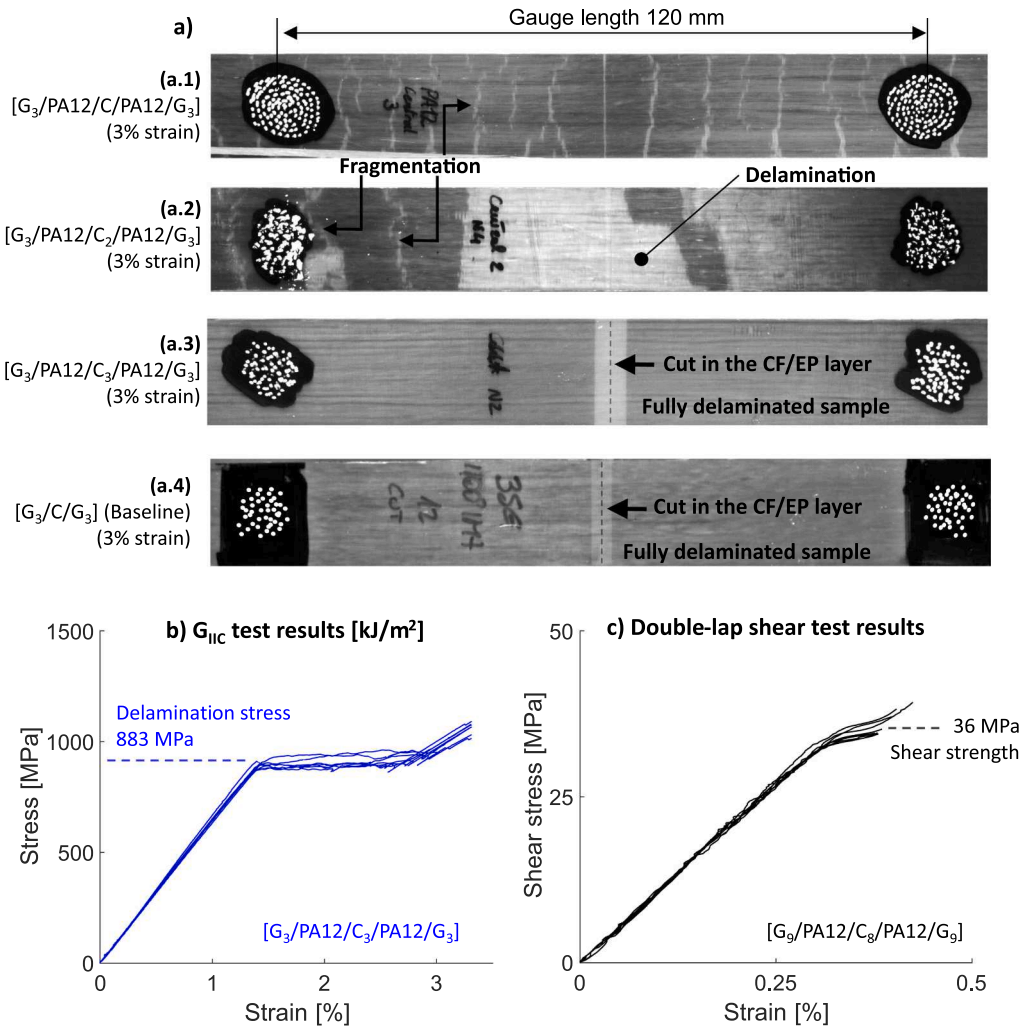

Fig. 4. (a) Appearance of the central-cut samples, (a.1) to (a.3) hybrids containing PA12 films and (a.4) non-interleaved configuration (baseline [14]), after the fracture toughness test (at 3% of strain). Experimental results of (b) mode II interlaminar fracture toughness (G_{IIC}) and (c) double-lap shear tests. The tests were performed on the hybrid composites interleaved with PA12 films. The material architectures are shown in Fig. 2 (a) and (b).

yielding behaviour before the final separation that should be linked to the ductile behaviour of the PA12 films.

According to the τ_s and G_{IIC} results (summarised in Table 5), we determined the parameters for designing the specimens used in the reparability study, satisfying equations (2.1) and (2.4). The minimum thickness for one GF/EP layer to avoid premature failure, according to equation (2.3), is 0.39 mm and the designed specimens have 0.47 mm thick GF/EP layers (see Table 5). The designed length of the CF/EP platelets is 50 mm, more than two times the ineffective length of the CF/EP layer (i.e. $L_{pc} = 20.8$ mm – see Table 5) to promote the contribution of the CF/EP platelets to high initial elastic modulus. No fracture of the platelets is expected as the G_{II} at CF/EP fracture (i.e. 6.3 kJ/m^2) is higher than the estimated G_{IIC} of the layer interfaces (i.e. 4.0 kJ/m^2) therefore equation (2.4) is fulfilled. This means that the CF/EP platelets should start delaminating from the GF/EP layers well before their fracture. We predicted 1.6% delamination initiation (i.e. knee-point) strain, which provides sufficient margin from the expected failure strain of the CF/EP layer (i.e. around the fibre failure strain 1.9% [14]). The selected and approved layups sequence for the reparability study is [G_3/PA12/C_3/PA12/G_3] with three prepreg plies in each layer interleaved with PA12 films (see Fig. 1 (a)).

4.2. Tensile test results of the specimens for the reparability study

The tests on the specimens made for the reparability study aimed to i) assess the presence of pseudo-ductility and the damage mode (i.e. stable delamination) and ii) characterise and correlate the measured mechanical parameters with the predicted ones reported in Table 5. Fig. 5 (a) shows the experimental stress–strain curves, and the measured mechanical parameters are summarised in Table 5 and compared with the predicted values. The initial elastic modulus E_0 was equal to 62 GPa and the knee-point occurred at 902 MPa of stress and 1.6% of strain. All the values were in line with the predicted ones (see Table 5). The specimens demonstrated excellent pseudo-ductility with high initial elastic modulus, high plateau stress, gradual transitions between the initial linear and the plateau stages and clear warning (i.e. stiffness degradation and change in appearance) before final failure.

After characterising the designed discontinuous interleaved hybrid laminates, the samples were damaged in the *first loading tests* (step 1) by straining them up to 2.8%. Then, they were re-loaded again during the *re-loading tests* (step 2), and the resulting elastic modulus E_d was around 35 GPa, meaning that the samples lost around 43% of their original elastic modulus because of delamination (see Fig. 5 (a)). It is worth

Table 5
Predicted and measured data used for designing the specimens of hybrid composites interleaved with PA12 films used for reparability tests. CoV in % is expressed in brackets below the mean values.

	Design parameter estimation tests (Section 4.1)		Tensile test on hybrid configuration [G_3/PA12/C_3/PA12/G_3] with CF/EP platelets (Section 4.2)								
	Mode II interlaminar fracture toughness	Shear strength at the GF/EP-CF/EP interfaces	Strain energy release rate at nominal CF/EP failure strain (1.6%)	Platelet length	Critical platelet length	Nominal thickness of the CF/EP layer	Nominal thickness of the GF/EP layer	Thickness of the full hybrid laminate	Initial elastic modulus	Knee-point stress	Knee-point strain
	G_{IIC} [kJ/m^2]	τ_s [MPa]	G_{II} [kJ/m^2]	L_p [mm]	L_{pc} [mm]	$t_{CF/EP}$ [mm]	$t_{GF/EP}$ [mm]	h [mm]	E_0 [GPa]	σ_{kp} [MPa]	ε_{kp} [%]
Predicted	–	–	6.3[c]	50	20.8[d]	0.29	0.47	1.22	59.6[e]	934[f]	1.6[g]
Test data	4.0[a] (5.7)	36[b] (5.4)	–	50	–	–	–	1.30 (2.6)	62 (3.7)	902 (4.1)	1.6 (4.9)

[a] From G_{IIC} estimation test on [G_3/PA12/C_3/PA12/G_3] with central-cut CF/EP layer.
[b] From double-lap shear strength estimation test on [G_9/PA12/C_8/PA12/G_9].
[c] From equation (2.4).
[d] Calculated through equation (2.1), using the measured $\tau_s = 36$ MPa.
[e] Nominal equivalent modulus of the hybrid laminate, calculated using the rule of mixture and the knock-down factor due to discontinuities in the CF/EP layer as described in [3].
[f] Calculated through equation (2.2), using the measured $G_{IIC} = 4.0$ kJ/m^2.
[g] Predicted knee-point strain: $\varepsilon_{kp} = \sigma_{kp}/E_0$.

highlighting that this value depends on the strain at which the *first loading tests* (step 1) were interrupted. One of the damaged specimens was opened and the type of interlaminar failure was assessed visually. Based on our limited observations, it seems that the layer interfaces experienced adhesive failure (i.e. the film separated from the CF/EP side and remained bonded mainly to the GF/EP side).

4.3. Reparability test results: Effect of temperature

The results of the tensile tests on the samples repaired at different temperatures and the same 0.7 MPa pressure are shown in Fig. 6 (a), (b) and (c) and summarised in Table 6. The repairing cycle performed at 165 °C was not effective in repairing delamination. The curves of the repaired samples (blue curves in Fig. 6 (a)) almost overlapped with the results of the re-loading tests (red curves) in the stress–strain diagram showing very early delamination at strains as low as 0.1%. Table 6 reports the initial elastic modulus after the repair, E_0^R, registered in the early stage of the test for this series. Although the value of E_0^R was close to the pristine value, the knee-point stress was at 78 MPa and the knee-point strain was at 0.1% both with high coefficient of variation. These mechanical properties confirmed the poor re-bonding of the CF/EP platelets to the GF/EP layers at 165 °C and rendered this repair temperature not suitable. The reason for this low repair performance is probably the fact that the TPP interleaves did not melt at the repairing temperature and therefore it was not possible to re-establish the bonding between the GF/EP and CF/EP layers. Samples of the T175 series were repaired at 175 °C. The tensile tests after the repairing cycle showed good recovery of the initial elastic modulus (i.e. η_E was up to 97%), but the knee-point occurred at 352 MPa and 0.7% of strain, with repairing efficiencies of only 42% and 39%, respectively. The lower knee-point stress and strain, compared to those from the pristine samples, were indicative of premature delamination in the samples due to incomplete re-bonding of the layers. This is in line with the fact that the repairing temperature was still slightly below the nominal melt temperature (178 °C) of the applied PA12 films. The series T185 exhibited excellent repair of delamination in the samples. The initial elastic modulus was fully recovered (i.e. 101%), and the knee-point occurred at stress and strain values close to those of the pristine sample data. The repairing

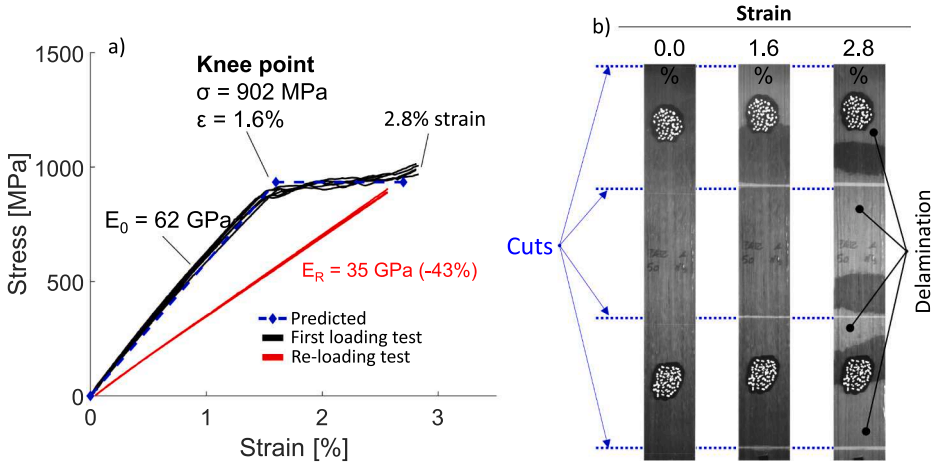

Fig. 5. (a) Stress–strain diagram of the tensile tests on specimens designed for the reparability study. (b) Damage stages in a typical sample. Delamination is visible from the outer surface of the samples (light areas).

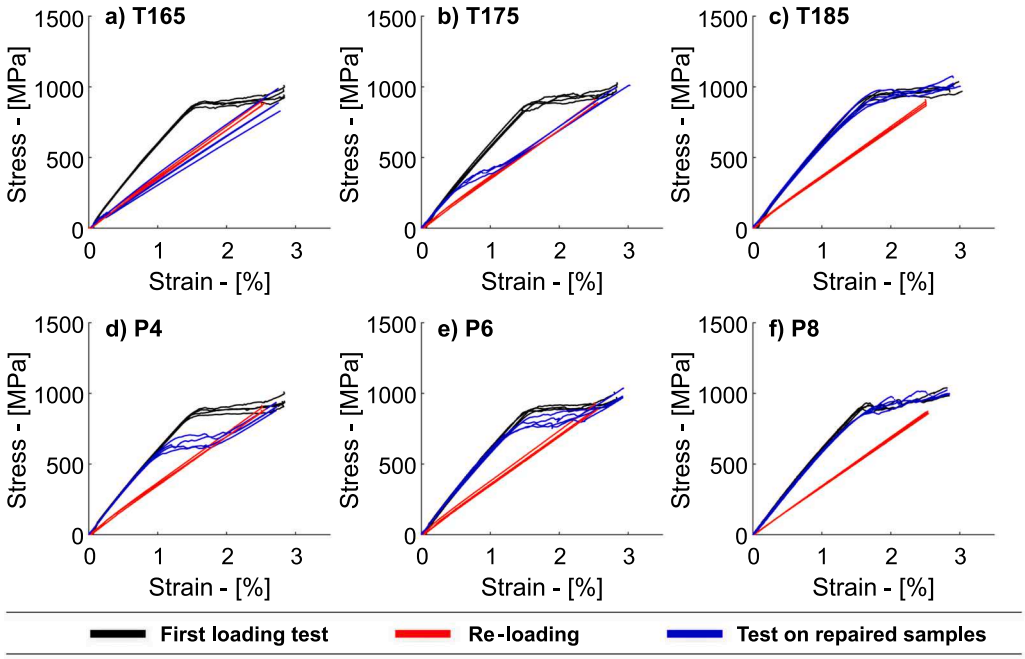

Fig. 6. Experimental stress–strain diagrams of the reparability tests. Please find the repairing parameters for the series in Table 6.

Table 6
Experimental data from reparability tests. CoV in % expressed in brackets below the mean values.

			First loading test (Step1)			Re-loading test (Step 2)	Test on repaired samples (Step 3)			Repairing efficiency (repaired/pristine)		
			Initial elastic modulus	Knee-point strain	Knee-point stress	Elastic modulus of delaminated samples	Initial elastic modulus	Knee-point strain	Knee-point stress	Initial elastic modulus	Knee-point strain	Knee-point stress
Lay-up sequence [G_3/PA12/C_3/PA12/G_3]	Temperature [°C]	Pressure [MPa]	E_0 [GPa]	ε_{kp} [MPa]	σ_{kp} [MPa]	E_d [GPa]	E_0^R [GPa]	ε_{kp}^R [MPa]	σ_{kp}^R [MPa]	η_E [–]	η_ε [–]	η_σ [–]
T165	165	0.7	60.8 (5.4)	1.53 (2.6)	866 (6.2)	33.4 (10.3)	56.2 (5.9)	0.12 (24.6)	78 (18.3)	93% (10.1)	8% (27.1)	9% (21.6)
T175	175	0.7	60.9 (4.4)	1.58 (5.3)	901 (2.6)	36.6 (0.3)	58.9 (1.7)	0.66 (14.1)	352 (12.5)	97% (2.8)	42% (10.2)	39% (10.9)
T185	185	0.7	60.8 (3.3)	1.70 (5.8)	952 (3.9)	35.0 (7.4)	61.5 (4.6)	1.57 (3.0)	895 (5.3)	101% (1.7)	92% (6.7)	94% (7.5)
P4	185	0.4	61.8 (1.6)	1.49 (2.4)	862 (2.0)	33.5 (1.7)	62.6 (1.0)	1.11 (7.4)	648 (6.9)	101% (2.0)	76% (8.8)	76% (7.7)
P6	185	0.6	59.2 (7.1)	1.52 (5.6)	840 (6.1)	33.8 (0.5)	61.2 (5.6)	1.27 (13.0)	719 (16.6)	104% (2.6)	84% (13.1)	85% (12.3)
P8	185	0.8	63.1 (3.4)	1.57 (2.2)	909 (1.3)	34.8 (2.6)	60.3 (1.7)	1.62 (8.3)	899 (6.3)	96% (3.1)	103% (7.8)	99% (5.3)

efficiency for the knee-point parameters was 92% and 94% for the stress and the strain, respectively. The reason for the excellent results must be the proper melting of PA12 films and the efficient re-bonding of the previously delaminated layers of the hybrid specimens.

4.4. Reparability test results: Effect of pressure

The test results of the specimen series repaired at different values of pressure in the autoclave are shown in Fig. 6 (d), (e) and (f). The P4 series exhibited a full recovery of the initial elastic modulus but the knee-point in the repaired samples was at 648 MPa, and 1.1% of strain, i.e. both values were reduced to 76% of the pristine data. At higher pressure, i.e. 0.6 and 0.8 MPa, the repairing efficiency was high for all investigated parameters. The knee-point for the P6 series occurred at around 85% of the original stress and strain values. In case of the P8 series, the mechanical parameters of the repaired samples were fully recovered, i.e. the repairing efficiency was 96% for the initial elastic modulus and around 100% for the knee-point stress and strain. These results clearly show that high pressure during the repairing cycle is beneficial for the recovery of mechanical properties after delamination.

5. Discussion

The specimens designed for the reparability study exhibited pseudo-ductile behaviour, characterised by a flat plateau due to stable delamination (Fig. 5 (a)). The stable delamination and the mechanical

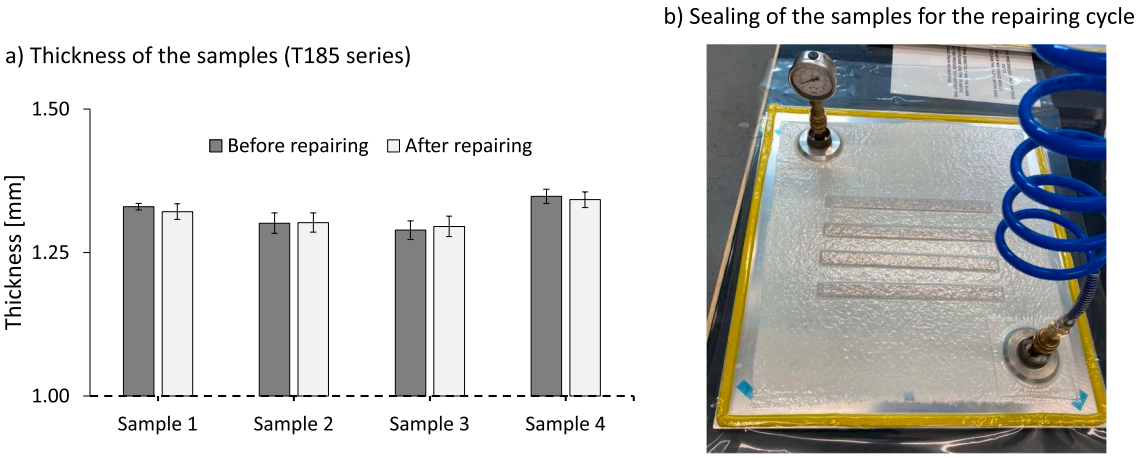

Fig. 7. (a) Thickness of the samples before and after the repair, (b) arrangement of the samples for the repairing cycles.

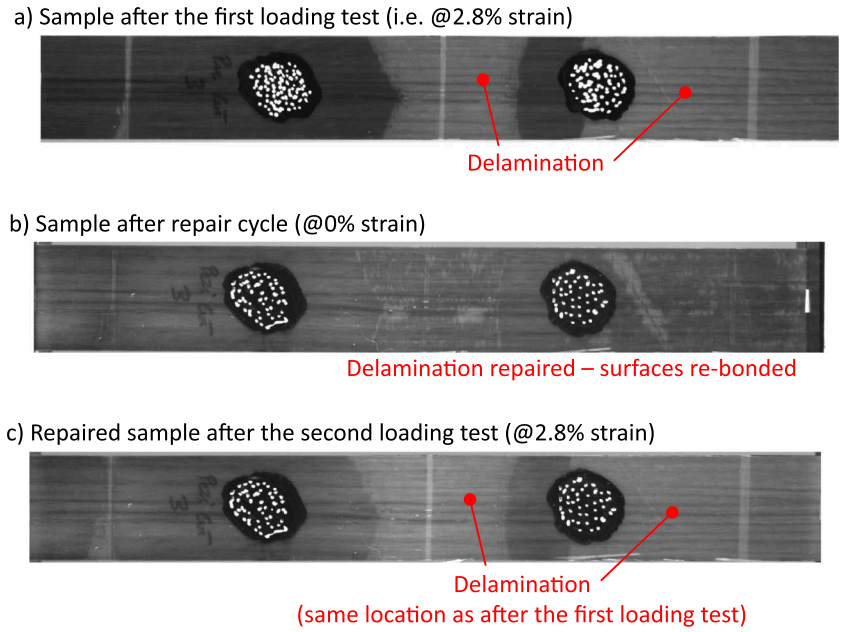

Fig. 8. Appearance of the samples (a) after the first loading test (stage 1), (b) after the repairing cycle and (c) after the second loading test (stage 3).

properties registered in the samples were in line with the predictions based on the estimated G_{IIC} and interfacial shear strength. The notable increase of G_{IIC} in comparison to the baseline (+100%) can be accounted to the PA12 TPP films. The strong bonding between PA12 and epoxy [36–38], and the ductile behaviour of the PA12 films are the most likely factors leading to the high G_{IIC} registered during the experiments. Based on our results, PA12 films can be considered as an excellent solution for toughening hybrid composites and enabling pseudo-ductility. The plateau stage was characterised by a slow spreading of delamination that started from the discontinuities in the CF/EP layer (see Fig. 5 (b)). Around 70–80% of the samples' surface delaminated during the *first loading tests* (step 1), interrupted at 2.8% of strain (see Fig. 8 (a)). The presence of delamination in the samples was visible to the naked eyes due to the translucency of the GF/EP layers. The delaminated zones looked lighter than the still bonded parts of the samples. This self-monitoring feature can be an additional benefit in certain critical applications and it was proposed earlier even for overload monitoring [39,40].

The repairing process restored the original overall appearance of the samples in all the parametric cases considered. It is worthwhile to mention that no traces of leakage were noticed and measured in the samples accountable to the repair cycles, even in case of cycles at high temperature and pressure. The visual inspection of the samples before and after the repair did not highlight traces of leakage. We also measured the thickness of the samples in the T185 series before and the after the repair but did not find any significant change. The results are reported in Fig. 7 (a). The low thickness of the thermoplastic film, i.e. 20 μm, reduced the risk of leakage during the repair as there was only a small volume available. The efficient sealing arrangement of the samples with some spacing between each other to improve the pressure distribution along the sides as well could also have prevented the thermoplastic from flowing out of the sample. The presence of the breather (white layer in Fig. 7 (b)) and the release film (transparent, not visible) made the pressure applied on the samples uniform also at the sides.

The typical sample reported in Fig. 8 (b) reflects the overall appearance of all the samples during all the steps of the experimental campaign. However, the mechanical performance of the samples depended on the actual repairing parameters used, which highly

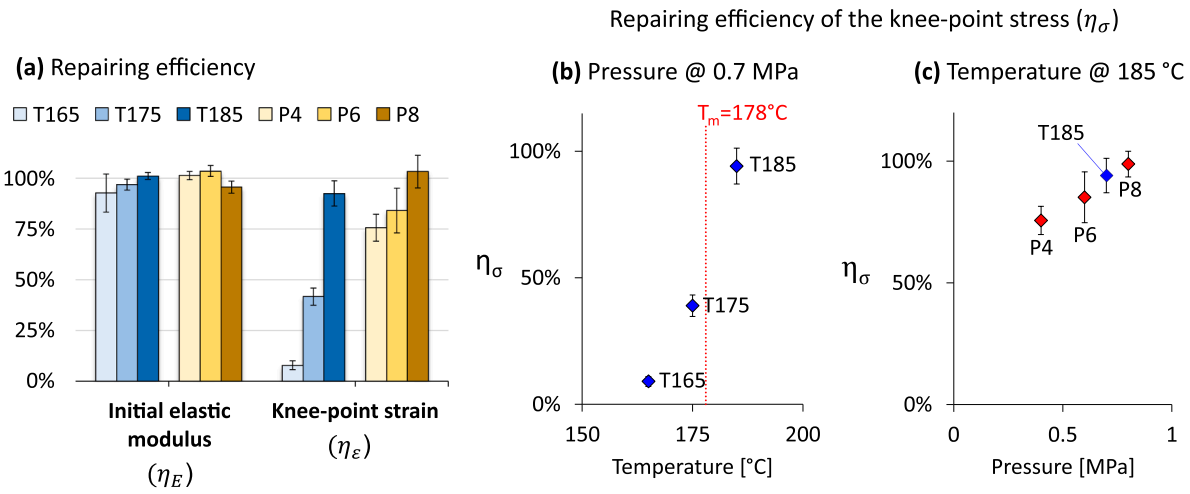

Fig. 9. (a) Repairing efficiency registered in the repaired material for the i) initial elastic modulus and ii) knee-point strain. (b) and (c) show the repairing efficiencies for the knee-point stress registered in the temperature and the pressure studies, respectively. T_m in (b) is the melting temperature of PA12.

affected the position of the knee-point on the stress–strain diagrams.

We performed the reparability study on discontinuous PA12 film interleaved CF/EP-GF/EP hybrid composite laminates with six different sets of parameters varying the temperature or the pressure of the repairing cycles (parameters are summarised in Table 4). The results showed that to maximise the repairing potential of the PA12 films, we needed to set the repairing temperature above their melting temperature (178 °C). The repairing efficiency for the knee-point was highly sensitive to the repairing temperature; in fact, it varied from around 40% in the T175 series to 95% in the T185 series (see Fig. 9). The higher repairing efficiency obtained with the T185 series can be attributed to the reduced viscosity of the PA12 films above the melting temperature. The low viscosity enabled better flow of the TPP material and allowed to completely wet and re-bond the delaminated surfaces.

The pressure study showed strong increase in repairing efficiency of the knee-point in the samples with the pressure set for the repairing cycles (see Fig. 9 (c)). Better repairing performances achieved with higher pressures must be related to the better penetration of the molten PA12 into the microstructure of the delaminated surfaces resulting in more complete wetting and finally better re-bonding after cooling. In some cases, the mechanical parameters evaluated for the repaired samples were higher than those measured with the pristine samples, i.e. repairing efficiency higher than 100%. It typically happened in the series repaired at temperature higher than the melting point of the thermoplastic films. In some of the cases it is most probably due to the scatter of the experimental data. It might also be the consequence of melting the PA12 interleaves during the repairing cycle (i.e. at 185 °C), unlike during the manufacturing cycle (at 125 °C). This latter possible explanation needs further investigation.

In most of the cases analysed (except for the T165 series), besides the partial or total recovery of mechanical properties, the samples preserved their pseudo-ductile behaviour after the repairing cycle, exhibiting the plateau generated by stable delamination. The results showed that discontinuous hybrid composites interleaved with PA12 films can restore their original tensile mechanical properties and pseudo-ductile behaviour if suitable repairing parameters are set.

6. Conclusions

This paper presented a detailed procedure for designing and characterising reparable pseudo-ductile interleaved discontinuous CF/EP-GF/EP interlayer hybrid composites. The polyamide 12 (PA12) films, interleaved between the CF/EP and GF/EP layers, were fundamental enablers for both pseudo-ductility and reparability in the hybrid composite. The effect of the film interleaves can be summarised in i) toughening the layer interfaces in the hybrid composites, ii) re-bonding delaminated surfaces in the damaged samples during a repair cycle. Reparability was effectively activated at temperatures above 178 °C by melting the TPP films and high pressure (i.e. 0.7 MPa) was applied to improve the bonding by enabling complete wetting of the delaminated surfaces by the molten PA12. The key findings reported in this paper are summarised here:

- Reparable discontinuous pseudo-ductile CF/EP-GF/EP hybrid composites were successfully designed and fabricated. The samples exhibited pseudo-ductile behaviour based on stable delamination starting from the designed discontinuities in the CF/EP layers. The repairing cycles in autoclave fully repaired delamination, exploiting the re-bonding ability of the PA12 films interleaved in the hybrid sample plates through phase changes.
- PA12 film interleaving increased the mode II interlaminar fracture toughness (G_{IIC}) of the hybrid composite plates from 2.0 kJ/m^2 (baseline) to 4.0 kJ/m^2. This notable improvement may enable pseudo-ductility in a range of new hybrid composite materials.
- Reparability was highly sensitive to the repairing temperature. To fully exploit the potential of PA12 films for reparability, we had to set the repairing temperature above their melting point.
- Higher pressure improved reparability as it helped the molten PA12 films to completely wet and re-bond the separated surfaces.
- The samples repaired at 185 °C and pressure at or above 0.7 MPa completely restored their original mechanical properties and preserved pseudo-ductility.

The tools provided here can be used to design and manufacture reparable pseudo-ductile hybrid composites relatively simply. Furthermore, the presence of PA12 films in hybrid composites is an effective solution for manufacturing delamination-resistant materials. The simple PA12 film interleaving technique may ease the introduction of reparable pseudo-ductile composites in large-scale industrial applications. The mechanical performance of the hybrid materials can be optimised and tailored by varying the design and repairing parameters. Future studies may be oriented to assess the effectiveness of PA12 films in repairing hybrid composites for multiple repairing cycles.

CRediT authorship contribution statement

Salvatore Giacomo Marino: Conceptualization, Methodology, Formal analysis, Investigation, Writing – original draft. **Gergely Czél:**

Conceptualization, Methodology, Resources, Writing – review & editing, Supervision, Project administration, Funding acquisition.

Declaration of Competing Interest

The authors declare that they have no known competing financial interests or personal relationships that could have appeared to influence the work reported in this paper.

Data availability

Data will be made available on request.

Acknowledgements

The research leading to these results has been performed within the framework of the *HyFiSyn* project and has received funding from the European Union's Horizon 2020 research and innovation programme under the *Marie Skłodowska-Curie* grant agreement No 765881. The research was also supported by the National Research, Development and Innovation Office (NRDI, Hungary) through grant OTKA FK 131882. The research reported in this paper is part of project no. BME-NVA-02, implemented with the support provided by the Ministry of Innovation and Technology of Hungary from the National Research, Development and Innovation Fund, financed under the TKP2021 funding scheme. Gergely Czél is grateful for funding through the Premium Postdoctoral Fellowship Programme and the János Bolyai Research Scholarship of the Hungarian Academy of Sciences. The work was supported by the ÚNKP-22-5-BME-323 New National Excellence Program of the Ministry for Culture and Innovation from the source of the National Research, Development and Innovation Fund.

References

[1] Czél G, Wisnom MR. Demonstration of pseudo-ductility in high performance glass/epoxy composites by hybridisation with thin-ply carbon prepreg. Compos Part A Appl Sci Manuf 2013;52:23–30. https://doi.org/10.1016/j.compositesa.2013.04.006.

[2] Bismarck A, Bacarreza O, Blaker J, Diao H, Grail G, Pimenta S, et al. Exploring routes to create high performance pseudo-ductile fibre reinforced composites. ICCM Int. Conf. Compos. Mater., vol. 2015-July, Copenhagen; 2015.

[3] Czél G, Jalalvand M, Wisnom MR. Demonstration of pseudo-ductility in unidirectional hybrid composites made of discontinuous carbon/epoxy and continuous glass/epoxy plies. Compos Part A Appl Sci Manuf 2015;72:75–84. https://doi.org/10.1016/j.compositesa.2015.01.019.

[4] Yu HN, Longana ML, Jalalvand M, Wisnom MR, Potter KD. Hierarchical pseudo-ductile hybrid composites combining continuous and highly aligned discontinuous fibres. Compos Part A Appl Sci Manuf 2018;105:40–56. https://doi.org/10.1016/j.compositesa.2017.11.005.

[5] Finley JM, Yu H, Longana ML, Pimenta S, Shaffer MSP, Potter KD. Exploring the pseudo-ductility of aligned hybrid discontinuous composites using controlled fibre-type arrangements. Compos Part A Appl Sci Manuf 2018;107:592–606. https://doi.org/10.1016/j.compositesa.2017.11.028.

[6] Swolfs Y, Verpoest I, Gorbatikh L. Recent advances in fibre-hybrid composites: materials selection, opportunities and applications. Int Mater Rev 2019;64:181–215. https://doi.org/10.1080/09506608.2018.1467365.

[7] Czél G, Pimenta S, Wisnom MR, Robinson P. Demonstration of pseudo-ductility in unidirectional discontinuous carbon fibre/epoxy prepreg composites. Compos Sci Technol 2015;106:110–9. https://doi.org/10.1016/j.compscitech.2014.10.022.

[8] Cohades A, Branfoot C, Rae S, Bond I, Michaud V. Progress in Self-Healing Fiber-Reinforced Polymer Composites. Adv Mater Interfaces 2018;5:1800177. https://doi.org/10.1002/admi.201800177.

[9] Kanu NJ, Gupta E, Vates UK, Singh GK. Self-healing composites: A state-of-the-art review. Compos Part A Appl Sci Manuf 2019;121:474–86. https://doi.org/10.1016/J.COMPOSITESA.2019.04.012.

[10] Chow WS, Mohd Ishak ZA. Smart polymer nanocomposites: A review. Express Polym Lett 2020;14:416–35. https://doi.org/10.3144/EXPRESSPOLYMLETT.2020.35.

[11] Pingkarawat K, Wang CH, Varley RJ, Mouritz AP. Self-healing of delamination cracks in mendable epoxy matrix laminates using poly[ethylene-co-(methacrylic acid)] thermoplastic. Compos Part A Appl Sci Manuf 2012;43:1301–7. https://doi.org/10.1016/j.compositesa.2012.03.010.

[12] Yuan YC, Yin T, Rong MZ, Zhang MQ. Self healing in polymers and polymer composites. Concepts, realization and outlook: A review. Express Polym Lett 2008;2:238–50. https://doi.org/10.3144/EXPRESSPOLYMLETT.2008.29.

[13] Marino SG, Mayer F, Bismarck A, Czél G. Effect of Plasma-Treatment of Interleaved Thermoplastic Films on Delamination in Interlayer Fibre Hybrid Composite Laminates. Polymers 2020;12:2834. https://doi.org/10.3390/polym12122834.

[14] Marino SG, Czél G. Improving the performance of pseudo-ductile hybrid composites by film-interleaving. Compos Part A Appl Sci Manuf 2021;142:106233. https://doi.org/10.1016/j.compositesa.2020.106233.

[15] Wang CH, Sidhu K, Yang T, Zhang J, Shanks R. Interlayer self-healing and toughening of carbon fibre/epoxy composites using copolymer films. Compos Part A Appl Sci Manuf 2012;43:512–8. https://doi.org/10.1016/j.compositesa.2011.11.020.

[16] Bilge K, Papila M. Interlayer toughening mechanisms of composite materials. Toughening Mech. Compos. Mater., Elsevier Inc.; 2015. p. 263–94.

[17] Asadi J, Golshan Ebrahimi N, Razzaghi-Kashani M. Self-healing property of epoxy/nanoclay nanocomposite using poly(ethylene-co-methacrylic acid) agent. Compos Part A Appl Sci Manuf 2015;68:56–61. https://doi.org/10.1016/J.COMPOSITESA.2014.09.017.

[18] Pingkarawat K, Bhat T, Craze DA, Wang CH, Varley RJ, Mouritz AP. Healing of carbon fibre-epoxy composites using thermoplastic additives. Polym Chem 2013;4:5007–15. https://doi.org/10.1039/c3py00459g.

[19] Pingkarawat K, Wang CHH, Varley RJJ, Mouritz APP. Mechanical properties of mendable composites containing self-healing thermoplastic agents. Compos Part A Appl Sci Manuf 2014;65:10–8. https://doi.org/10.1016/j.compositesa.2014.05.015.

[20] Varley RJ, Charve F. EMAA as a healing agent for mendable high temperature epoxy amine thermosets. Compos Part A Appl Sci Manuf 2012;43:1073–80. https://doi.org/10.1016/J.COMPOSITESA.2012.01.018.

[21] Pingkarawat K, Wang CHH, Varley RJJ, Mouritz APP. Effect of mendable polymer stitch density on the toughening and healing of delamination cracks in carbon-epoxy laminates. Compos Part A Appl Sci Manuf 2013;50:22–30. https://doi.org/10.1016/j.compositesa.2013.02.014.

[22] Varley RJ, Parn GP. Thermally activated healing in a mendable resin using a non woven EMAA fabric. Compos Sci Technol 2012;72:453–60. https://doi.org/10.1016/j.compscitech.2011.12.007.

[23] Magyar B, Czigany T, Szebényi G. Metal-alike polymer composites: The effect of inter-layer content on the pseudo-ductile behaviour of carbon fibre/epoxy resin materials. Compos Sci Technol 2021;215:109002. https://doi.org/10.1016/J.COMPSCITECH.2021.109002.

[24] Szebényi G, Magyar B, Czigany T. Achieving Pseudo-Ductile Behavior of Carbon Fiber Reinforced Polymer Composites via Interfacial Engineering. Adv Eng Mater 2021;23:2000822. https://doi.org/10.1002/ADEM.202000822.

[25] Keller MW, Crall MD. Self-healing composite materials. Compr Compos Mater II 2018;6:431–53. https://doi.org/10.1016/B978-0-12-803581-8.10026-8.

[26] Fakirov S. Editorial corner – a personal view once more on the proper use of terms and definitions: This time about the term 'self-healing'. Express Polym Lett 2021;15:88. https://doi.org/10.3144/expresspolymlett.2021.9.

[27] Meure S, Varley RJ, Wu DY, Mayo S, Nairn K, Furman S. Confirmation of the healing mechanism in a mendable EMAA–epoxy resin. Eur Polym J 2012;48:524–31. https://doi.org/10.1016/J.EURPOLYMJ.2011.11.021.

[28] Pingkarawat K, Dell'Olio C, Varley RJ, Mouritz AP. Poly(ethylene-co-methacrylic acid) (EMAA) as an efficient healing agent for high performance epoxy networks using diglycidyl ether of bisphenol A (DGEBA). Polymer (Guildf) 2016;92:153–63. https://doi.org/10.1016/J.POLYMER.2016.03.054.

[29] Varley RJ, Craze DA, Mouritz AP, Wang CH. Thermoplastic healing in epoxy networks: Exploring performance and mechanism of alternative healing agents. Macromol Mater Eng 2013;298:1232–42. https://doi.org/10.1002/mame.201200394.

[30] Zhang T, Yasaee M. Influence of thermoplastic interleaves and its healing effect on the failure mechanisms of open-hole notched composite laminates. Compos Sci Technol 2022;227:109597. https://doi.org/10.1016/J.COMPSCITECH.2022.109597.

[31] Ammar M, Haleem A, Javaid M, Bahl S, Verma AS. Implementing Industry 4.0 technologies in self-healing materials and digitally managing the quality of manufacturing. Mater Today Proc 2022;52:2285–94. https://doi.org/10.1016/J.MATPR.2021.09.248.

[32] Pegoretti A. The way to autonomic self-healing polymers and composites. Express Polym Lett 2009;3:62. https://doi.org/10.3144/EXPRESSPOLYMLETT.2009.9.

[33] Wisnom MR. On the Increase in Fracture Energy with Thickness in Delamination of Unidirectional Glass Fibre-Epoxy with Cut Central Plies. J Reinf Plast Compos 1992;11:897–909. https://doi.org/10.1177/073168449201100802.

[34] Wisnom MR, Jones MI. Size effects in interlaminar tensile and shear strength of unidirectional glass fibre/epoxy. J Reinf Plast Compos 1996;15:2–15. https://doi.org/10.1177/073168449601500101.

[35] Czél G, Jalalvand M, Wisnom MR. Hybrid specimens eliminating stress concentrations in tensile and compressive testing of unidirectional composites. Compos Part A Appl Sci Manuf 2016;91:436–47. https://doi.org/10.1016/j.compositesa.2016.07.021.

[36] Deng S, Djukic L, Paton R, Ye L. Thermoplastic-epoxy interactions and their potential applications in joining composite structures - A review. Compos Part A Appl Sci Manuf 2015;68:121–32. https://doi.org/10.1016/j.compositesa.2014.09.027.

[37] Gorton BS. Interaction of nylon polymers with epoxy resins in adhesive blends. J Appl Polym Sci 1964;8:1287–95. https://doi.org/10.1002/app.1964.070080319.
[38] Zhong Z, Guo Q. Miscibility and cure kinetics of nylon/epoxy resin reactive blends. Polymer (Guildf) 1998;39:3451–8. https://doi.org/10.1016/S0032-3861(97)10237-3.
[39] Rev T, Jalalvand M, Fuller J, Wisnom MR, Czél G. A simple and robust approach for visual overload indication - UD thin-ply hybrid composite sensors Compos Part. A Appl Sci Manuf 2019;121:376–85. https://doi.org/10.1016/J.COMPOSITESA.2019.03.005.
[40] Wisnom MR, Potter K, Czél G, Jalalvand M. Strain overload sensor. GB2544792B; 2020.